Internal Pressures and Pressure Gradients in Mass-Impregnated HVDC Cables during Current Cycling

M. Runde, E. Jonsson, N. Magnusson, and **K. T. Solheim**
SINTEF Energy Research,
NO-7465 Trondheim, Norway

ABSTRACT

The internal pressures in the insulation of two 5-m long pieces of a state-of-the art mass-impregnated non-draining subsea cable have been measured under load current cycling at ambient temperatures ranging from 3 to 37 °C. Thermal expansion of the mass gives in some cases rather extreme internal pressures (>30 bar) and radial pressure gradients (>1.5 bar/mm) in the insulation. This leads to an outwardly directed flow of mass during loading. After a load turn-off, the pressure drops rapidly. Values below 100 mbar were measured in the inner parts of the insulation. The backflow of mass proceeds much slower because the pressure gradient now is smaller. Such a radial redistribution of the mass and the low pressures are assumed to influence the dielectric properties of the insulation as the risk of creating harmful shrinkage cavities is believed to increase. For all the investigated ambient temperature levels the internal pressure in the insulation became around 1 bar or less when isothermal conditions were reached after the load turn-offs. This demonstrates that thermal expansion and contraction of the mass are not the sole mechanisms determining the internal pressures in such cables. Other, still unidentified phenomena are also contributing.

Index Terms — **dielectric liquids, HVDC insulation, impregnated insulation, power cable insulation, pressure effects, underwater cables**

1 INTRODUCTION

TO ENSURE a reliable electrical power delivery and to facilitate interconnections of asynchronous power grids, the demand for subsea cables has been steadily increasing over the last decades. For long sea crossings, high voltage direct current (HVDC) links using mass-impregnated non-draining (MIND) cables have been the preferred technology [1].

The purpose of the present work is to provide quantitative information about internal pressures, pressure distributions and pressure dynamics of MIND cable insulation. This is believed to be essential for obtaining a better understanding of the behavior of the insulation system of such cables, in particular its capabilities and limitations during high current load and rapid load changes. There are reasons to suspect that incomplete knowledge of various pressure related phenomena causes the real capacity and operational flexibility of MIND cables not to be fully exploited.

The electrical insulation consists of up to around 250 layers of tape of paper or polypropylene-laminated paper impregnated with a high viscosity oil (the "mass"). The thickness of the insulation is around 20 mm for the highest available voltage ratings, at present in excess of 500 kV.

The cables are manufactured by first lapping the paper tapes onto the conductor, then transferring the several kilometer-long batch into a large impregnating vessel and immersing it in mass at a temperature well above 100 °C and under a few bars pressure. After several weeks the mass has filled the pores in the paper, the butt gaps (i.e., the 2–4 mm wide helical channels between adjacent paper tapes), and the space between the conductor strands.

The temperature of the impregnation vessel is then very slowly reduced. The mass has a volumetric thermal expansion coefficient around 10 times higher than the paper, so when cooling down the cable the mass contracts more than the paper and the conductor. Hence, more mass needs to penetrate the paper layers to keep the entire cable cross-section fully impregnated. However, at some point – presumably around 50–55 °C – the viscosity of the mass becomes so high that the impregnation virtually ceases. When lowering the temperature further, the contraction of the mass continues, causing the pressure in the insulation to drop. At around 30–40 °C a lead sheath is extruded on, sealing the insulation off. Further cooling causes the internal pressure to fall even more, and below a certain temperature it is assumed that the mass deficit leads to formation of shrinkage cavities in the insulation. Hence, the high viscosity and the large coefficient of thermal expansion of the mass result in that MIND cables have a low internal pressure and probably also voids or cavities in the insulation when the temperature is low [2]. The low gas pressure inside the cavities causes their dielectric strength to be lower than in the rest of the insulation, at least for cavities of certain sizes.

The type test for MIND cables [3] includes a load cycling test in

Manuscript received on X XXX 2019, in final form X XXXX, accepted xx Month 20yy. Corresponding author: M. Runde.

This is the accepted version of an article published in IEEE transactions on dielectrics and electrical insulation
http://dx.doi.org/10.1109/TDEI.2019.008522

5 °C ambient. Partial discharges igniting in the shrinkage cavities as the cable cools down after load turn-offs in some cases develop into a complete breakdown, and the test fails [4, 5]. Even though the service record for MIND subsea cables is excellent, with nearly all failures being caused by external mechanical impacts (trawl doors, anchors etc.), it is evident that the internal pressure in the insulation influences the cable's ability to sustain high dielectric stresses.

The internal pressure and the pressure dynamics of MIND cables are affected by many more factors than thermal contraction and viscosity of the mass. These include manufacturing parameters such as the mechanical tension applied to the paper tapes during lapping, material properties such as the permeability of the paper, ambient conditions such as the pressure exerted by the surrounding seawater, operational conditions such as the current rating and current ramping speed, and others.

A MIND cable design feature deserving particular mention in this context is the steel tapes that are wound on the outside of the lead sheath. Their purpose is to provide a compressive force and prevent high internal pressures during high load from permanently deforming the cable.

Despite the obvious importance of the internal pressure and pressure dynamics for the dielectric properties of subsea MIND cables, hardly any pressure measurements are reported in the open literature. A few articles provide interesting but predominantly qualitative descriptions about the behavior of the mass-impregnated insulation [5–8]. Evenset et al. have carried out idealized, small-scale experiments concentrating on low pressures and formation of cavities [9]. Modelling work has indicated that both very low (nearly vacuum) and high pressures (>10 bar) can be expected during load cycling [7, 10]. A review summarizes the current understanding of cavity formation and discusses pressure gradients and radial mass flow in some detail [2]. Numerical modelling of the electric field and the dielectric strength of cavities formed in the butt gaps [11, 12], as well as of how internal and external pressures and temperatures affect the maximum cable current rating [13] have been carried out. Recent work has studied the behavior of MIND cable insulation under different temperatures by means of partial discharge measurements [14, 15].

The present work reports measurements of internal pressure in the insulation of two 5–m long pieces of a state-of-the art MIND subsea cable. The pressure was recorded in the conductor and just underneath the lead sheath, i.e., on both sides of the insulation layer, under load current cycling at different ambient temperatures.

2 TEST SETUP

2.1 CABLE END SEALINGS

The test objects were two 5-m long sections cut from longer lengths of a 1600 mm^2 subsea MIND cable rated for 525 kV DC. The insulation consists of Kraft paper tapes impregnated with the T2015 compound normally used for this purpose. The cable where the samples were taken from has previously only been used for dielectric tests; it has not carried load currents.

Regarding the phenomena studied here, a MIND cable in service can be assumed to be infinitely long, without any axial flow of mass or any axial relative movements between the different layers of the cable, and with the insulation and conductor sealed off from the environment. When doing measurements on short samples, it is crucially important to use cable terminations / end caps that as much as possible imitate such conditions.

Figure 1. End cap used to seal off the ends of the 5-m long MIND cable samples used in the present study. It was machined out of a Ø=150 mm brass cylinder.

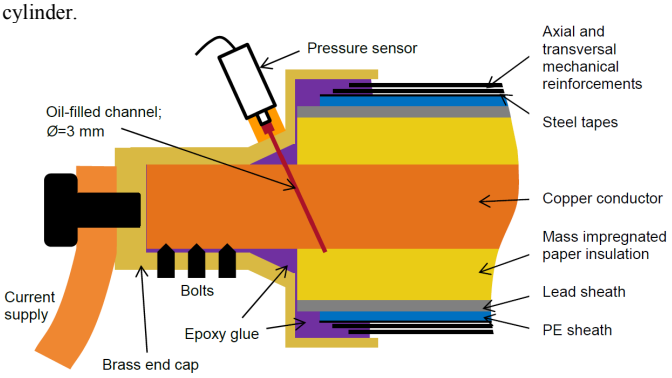

Figure 2. End cap and pressure sensor mounted on the MIND cable sample (schematic and not entirely to scale). Two 300 mm^2 copper cable lugs were connected at the far-left end of the cap for supplying current.

Figure 1 shows one of the brass end caps used, and Figure 2 shows a cross-sectional drawing of the end cap mounted on the cable sample.

The steel bolts fix the conductor to the end cap and do also ensure that a good electrical contact is established between the conductor and the grooved inner wall on the side opposite to the bolts. Epoxy glue (*Stycast 2850FT/24LV*) keeps both the axial and radial mechanical reinforcements and the steel tapes in place and prevents any relative axial and tangential movements between the different parts/layers of the cable. (Overall thermal expansion of the cable is still possible.) The epoxy also seals off the end of the mass-impregnated paper insulation, preventing mass from flowing in the radial direction across the end surface of the insulation. The epoxy is an electric insulator, so applied current cannot take parallel paths by going through the lead sheath or the steel reinforcements.

Putting on the end caps inevitably means cutting the cable and thereby exposing the end face of the insulation and the conductor to ambient air, but the exposure time was limited to a few minutes. The mounting of the caps started by removing all layers outside the lead sheath in a stepwise manner. The surfaces were then carefully cleaned and roughened to improve the adhesion of the epoxy. The inner parts (lead, insulation and conductor) were then cut, and a rapidly curing glass fiber reinforced polyester compound was applied to seal the end surface, see Figure 3.

This is the accepted version of an article published in IEEE transactions on dielectrics and electrical insulation
http://dx.doi.org/10.1109/TDEI.2019.008522

Figure 3. Cable end with the outer layers stepwise removed and cleaned. A polyester padding temporarily covers the end surface of the insulation and the conductor, preventing air ingress.

Then, after sawing through the lead sheath and the insulation around the conductor circumference about one centimeter from the edge of the PE sheath, the outermost 10 cm of lead and mass-impregnated paper could be pulled off, exposing the conductor and a new fresh cut of the insulation. The cable sample was then immediately hoisted up to a vertical position and carefully lowered into a brass end cap filled with liquid (i.e., un-cured) epoxy. The bolts were tightened, and the assembly was left to cure overnight in the vertical position with its lower end resting on the floor. The day after, the process was repeated to mount the second end cap at the other end. Figure 4 shows an end cap assembly after curing.

2.2 PRESSURE SENSOR FITTING

Four pressure sensors (*GE Unik 5000* series) were attached to each cable; one in each of the end caps and two at the mid-section.

The sensors at the end caps were mounted with the intention of measuring the pressure in the conductor / innermost layers of the insulation without at the same time making a radial channel through the insulation that would "short-circuit" any radial pressure differences. As indicated in Figure 2, a 3-mm hole was drilled through the end cap, the epoxy and through the conductor, and was then filled with warm mass. The threaded end of the sensor was mounted in the brass socket and firmly tightened.

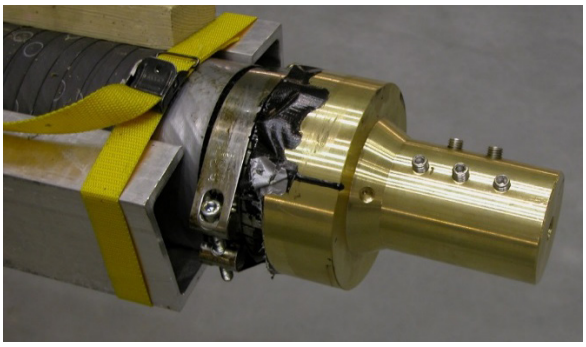

Figure 4. One of the end caps after gluing, but before removing the U-shaped aluminum supporting bars. The threaded hole for the pressure sensor brass socket is seen at the slanting surface.

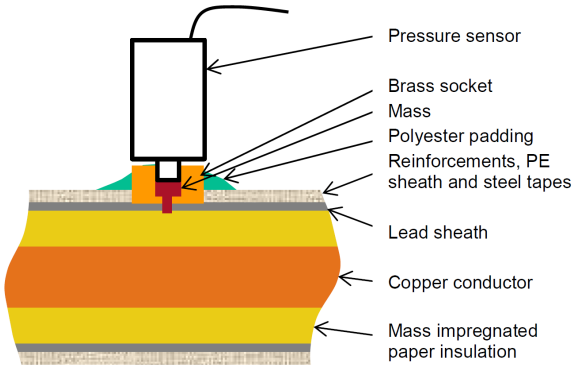

Figure 5. Pressure sensor assembly for measuring the pressure under the lead sheath.

The pressure sensors at the mid-section of the cable samples were mounted in threaded holes of brass sockets that were soldered directly onto the lead sheath, see Figure 5. A 3-mm diameter hole drilled through the bottom of the socket, the lead sheath and a little into the insulation was filled with warm mass. Hence, these sensors measure the pressure just under the lead sheath. A glass fiber reinforced polyester padding was applied to provide mechanical support to the assembly.

The pressure sensors have a 0–70 bar or 0–50 bar range, measuring absolute pressure. The nominal accuracy is 0.2% of their full-scale value, corresponding to 140 mbar for the 70-bar version. Deviations in the 5-V sensor supply voltage and the accuracy of the voltage measurements directly influence the precision. Tests where the sensors were attached to an evacuated chamber, estimate the error to less than 30 mbar for measurements at atmospheric pressures and below.

2.3 TEMPERATURE CONTROL

One of the cable samples was equipped with an arrangement for controlling its ambient temperature (i.e., the cable surface temperature). A heating/cooling machine circulated a liquid in copper pipes that had been wound onto the cable surface and embedded in an around 5-cm thick layer of a polymer compound of high thermal conductivity [14]. Sheets of polymer foam were wrapped around the compound to thermally insulate this test object from ambient. The temperature of the circulating liquid could be set to any appropriate level for such cables.

The other test object had no such temperature control. The current cycling was carried out with the cable simply kept in a laboratory environment at (a somewhat fluctuating) room temperature.

Temperatures were recorded by means of thermocouples. These measured the air temperature in the laboratory, the surface temperature of the end cups, and the cable surface temperature at several positions. Pressures and temperatures were recorded every 20 min for the entire duration of a test.

3 RESULTS

3.1 LOAD CYCLING IN ROOM TEMPERATURE

The cable without external temperature control was subjected to ten load cycles, each consisting of 3–4 days

This is the accepted version of an article published in IEEE transactions on dielectrics and electrical insulation
http://dx.doi.org/10.1109/TDEI.2019.008522

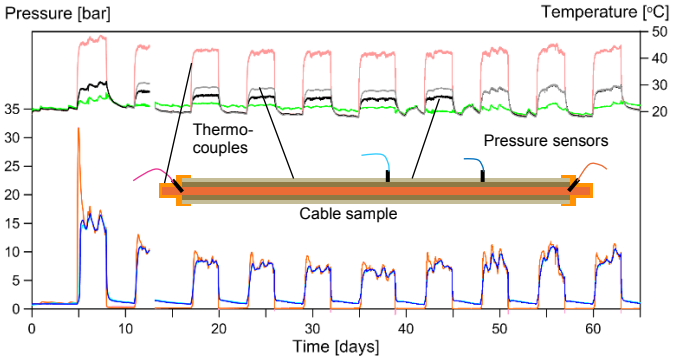

Figure 6. Pressures (lower plots) and temperatures (upper plots) recorded during 65 days of load current cycling. Light and dark orange lines (largely overlapping) are pressures in the conductor at the ends of the cable sample, whereas light and dark blue lines are pressures under the lead sheath at the locations indicated in the cable drawing inset. Black and grey lines are surface temperatures of the cable, pink is the temperature at an end cup, and the green curve shows the air temperature in the room. (A brief disruption occurred on day 12.)

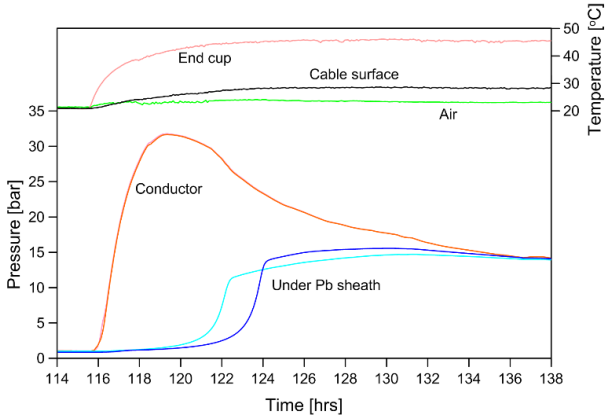

Figure 7. A 24-h excerpt from days 5 and 6 of the plots in Figure 6.

carrying the rated load current of 1400 A and 3–4 days with no current passed. Figure 6 shows pressure and temperatures recorded during this test. The current on and off periods are easily deduced from the pressure and temperature profiles.

Other heat cycling experiments running in the same laboratory caused the air temperature in periods to vary, and to reach rather high values; around 27 °C during the first load cycle, see the green curve in Figure 6. The internal pressure of MIND cables is sensitive to even modest changes in ambient temperature. For example, during cycles no. 1 and 8 the air temperature fluctuated with 1–2 °C. This resulted in internal pressure variations as large as 3–4 bar.

The temperature measurements on the cable surface are not very accurate, as a good thermal contact between the thermo-couples and the yarn was difficult to obtain. Moreover, the thermocouples easily loosened and had to be re-attached. These are the reasons for the intervals with deviations between the two cable surface temperature recordings (the grey and black lines).

The temperature at the brass end cap is assumed to correspond approximately to the conductor temperature. It never exceeds 55 °C, so the cable is not operating outside its rating. At full load, the cable surface temperature is typically around 16 °C lower than the end cap or conductor temperature, which is about as expected for this cable.

The pressure sensors give mutually consistent readings. The two attached to the cable ends measuring pressure in the conductor give virtually overlapping recordings almost throughout the entire campaign (light and dark orange lines of Figure 6), indicating a good axial pressure exchange through the conductor.

To a considerable extent, the same applies for the two sensors recording pressure at the outside of the insulation layer / under the lead sheath, see the light and dark blue lines. They give similar outputs, but as will be clear from plots showing more details than Figure 6, the curves are not overlapping. This indicates that the longitudinal pressure exchange here is poorer than through the conductor.

At the start of the first load cycle, the pressures measured at the conductor rose rapidly and exceeded 32 bar after around three hours, see Figure 7. The pressure under the lead sheath was at this point still essentially unchanged, but a few hours later it started to increase. Hence, for a short while there was a pressure difference of more than 30 bar across the insulation. This pressure gradient gradually levelled out, and after about 20 h it disappeared, while the temperature gradient across the insulation of course persisted because current was still flowing. Both pressure profiles obtained from under the lead sheath have a pronounced, strange kink at some 12–14 bar. No explanation for this has been found.

Figure 8 shows temperatures and pressures when the load was turned off for the first time, the three days without load and at the start of the second cycle.

The pressure variations during day 7 were caused by changes in the air temperature. After load turn-off, the pressure dropped rapidly. Over a little more than one hour, the pressure inside the conductor fell from approximately 15 bar to less than half a bar. The pressure under the lead sheath also dropped, but not as fast and not as much. After the cable reached isothermal conditions after a day or so, a modest pressure difference remained across the insulation.

At the start of the second load cycle, the pressure rose rapidly as in the first cycle. However, one feature of the pressure

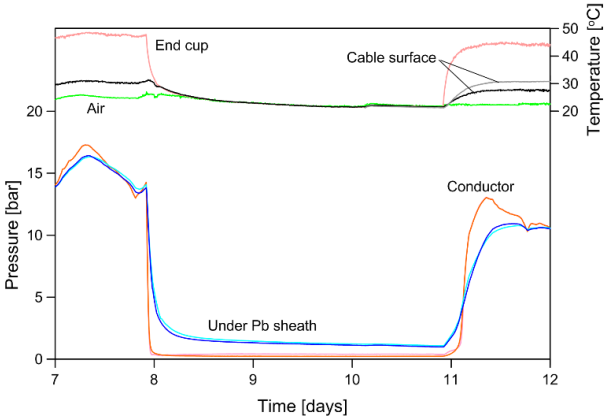

Figure 8. Pressures and temperatures recorded at the end of the first load cycle and one day into the second. (Note that the scaling on the pressure axis differs from Figures 6 and 7.) The cable surface temperature recordings were overlapping up to day 11, when one of the thermocouples had to be re-mounted.

This is the accepted version of an article published in IEEE transactions on dielectrics and electrical insulation
http://dx.doi.org/10.1109/TDEI.2019.008522

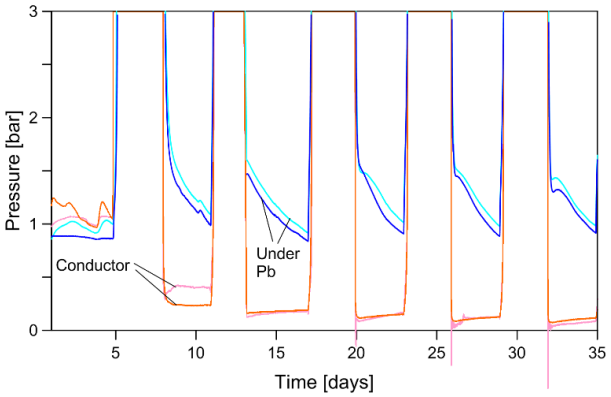

Figure 9. Pressures from the first five cycles, with the vertical axis scaling expanded to display the low pressures during the no-load phases of the cycles.

recordings from the first cycle was clearly different from the second and the other cycles that follow: The maximum pressure in the conductor observed in cycles 2–10 was in the range 8–13 bar, thus far lower than in the first cycle and also less different from the pressure recorded under the lead sheath. Thus, the large >30 bar pressure gradient across the insulation was only seen early in the first cycle.

Figure 9 zooms in on the pressure profiles obtained during the no-load parts of the first five cycles. Before the first cycle, all four sensors showed a pressure of around 1 bar. During the three-day periods without loading the pressure underneath the lead sheath slowly dropped from around 1.5 to 1 bar. The rate of pressure drop was fairly constant over the three days, also after the temperature gradient had faded out after the first day.

The pressure at the conductor was considerably lower, typically in the 100–200 mbar range in the interval shown in Figure 9; in later cycles it became as low as 50–60 mbar. It usually increased a little over the three-day period without load.

The average of the measured pressures in the cable at the end of each of the no-load periods was just half of what it was before current was applied for the first time, even though the thermal conditions were identical (i.e., room temperature throughout the cable cross-section).

One of the sensors that measured the pressure in the conductor gave readings corresponding to a negative pressure immediately after nearly all current turn-offs, see Figures 6 and 9. A detailed examination revealed that the negative values comprised from one to three data samples (i.e., 20–60 min) each time, and that values as low as –1 bar were recorded.

3.2 LOAD CYCLING AT DIFFERENT AMBIENT TEMPERATURES

As stated earlier, the other test object had arrangements for controlling the cable's surface temperature. Before the start of the test the cable had been stored for months at room temperature. The internal pressure was then around atmospheric (i.e., 1 bar). The temperature of the liquid circulating in the copper pipes wound around the cable was then set to 1 °C. After four weeks it was increased to 8 °C and then every three weeks raised another 7 °C until it reached 36 °C.

The load cycling on a new temperature level was initiated 24 h after the temperature was raised; this to allow the cable to reach isothermal conditions. Each cycle consisted of three days at rated load current and four days with the current turned off. Hence, three load cycles were carried out at each temperature level (except at 1 °C which had four cycles). After completing the three cycles at 36 °C, the temperature of the cooling liquid was set to 8 °C and the test terminated a few weeks later without any further load cyclings.

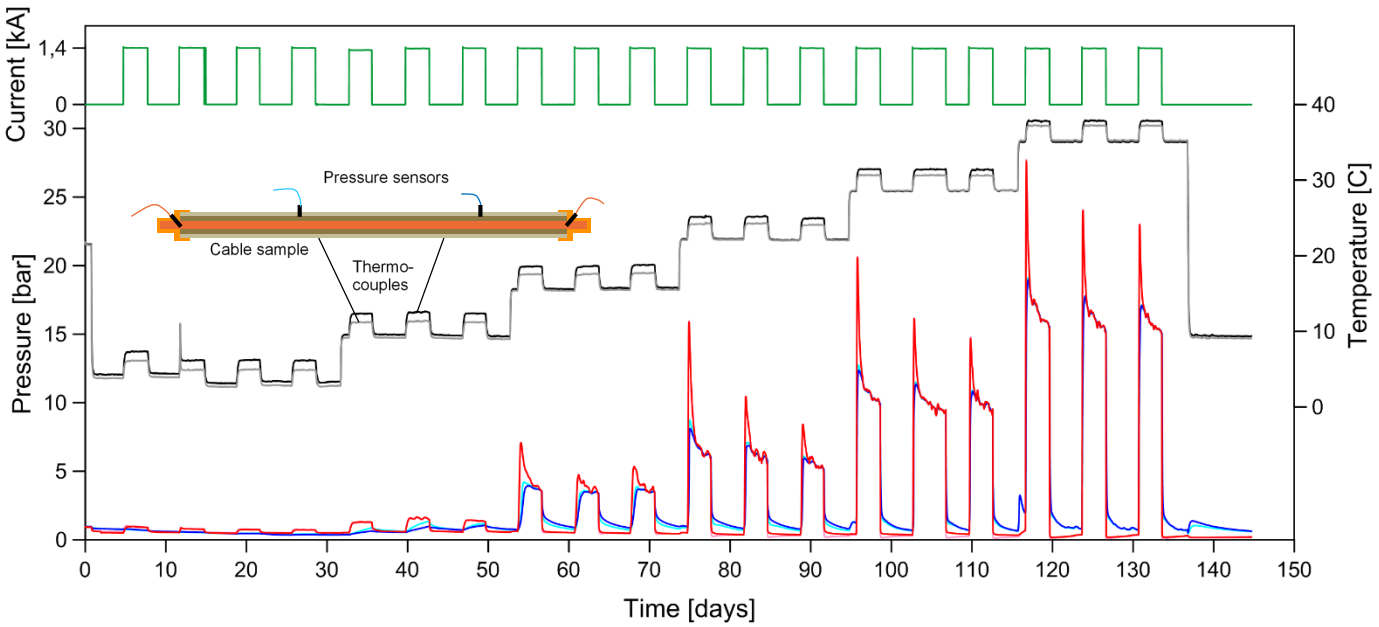

Figure 10. Temperatures, internal pressures and current during 21 weeks of load cycling at different ambient temperatures. Red and orange lines (often overlapping) are pressures in the conductor obtained at the ends of the cable sample, whereas light and dark blue lines show pressures under the lead sheath at the locations indicated in the cable drawing inset. Black and grey lines are thermocouple readings from the surface of the cable at the positions indicated. (Initial temperature control difficulties caused a little too high temperatures the first 11 days and a brief temperature overshoot at the end of this period. The load turn-off in cycle no. 15 came one day late.)

This is the accepted version of an article published in IEEE transactions on dielectrics and electrical insulation
http://dx.doi.org/10.1109/TDEI.2019.008522

Figure 10 shows the load current profile, the recorded internal pressures and cable surface temperatures over the 21 weeks the experiment lasted.

As can be seen from the temperature profiles, the circulating liquid was not able to maintain a perfectly constant cable surface temperature. Ohmic dissipation in the conductor caused the surface temperature to become up to some 3–4 °C higher with load than without. Like for the other test object, the thermocouple readings deviated somewhat, and changes in air temperature over the day sometimes caused minor internal pressure fluctuations.

Also for this test the sensors measuring pressure in the conductor at both ends of the cable gave essentially overlapping readings, whereas the two sensors that recorded pressure under the lead sheath differed somewhat, although they clearly showed the same trend.

Starting to circulate liquid at 1 °C at the beginning of the test caused the pressure to drop. During the 31 days at this temperature it continued to decline slowly, interrupted by a 0.3–0.5 bar temporary rise in the conductor pressures during the on-load periods. The pressure under the lead sheath was virtually unaffected by the current loading.

This changed as the ambient temperature was stepped up to higher levels. During current loading the pressure rose both under the lead sheath and in the conductor, and the amplitudes became higher at higher ambient temperatures. The pressure in the conductor peaked at 27.5 bar on day 116.

The pressure changes following a load turn-on was faster at higher ambient temperatures. Fig. 11 shows 24-h extracts of Figure 10 zooming in on the first load turn-on after the temperature of the circulation liquid had been raised to 15 and 36 °C, respectively. In the first case the internal pressure in the conductor reached its maximum value after around 10 h, whereas with the higher ambient temperature it took only about 2.5 h. The pressure under the lead sheath also changed more rapidly at higher temperatures.

The internal pressure during current loading clearly increased with increasing ambient temperature level. The internal pressure after the current was turned off did not show a similar correlation with temperature. A couple of days into the no-load parts of the cycling the internal pressure was always around atmospheric or below.

Concerning the other characteristics of the pressure profiles, these were similar to those observed in the other experiment:

- When turning on the load current the pressure increase came faster in the conductor than under the lead sheath, resulting in a large pressure gradient across the insulation.
- The maximum value of the pressure was in most cases significantly higher in the first load cycle on a new temperature level, than in the second and third.
- Some time into the loading part of the cycle, the pressure gradient disappeared, even though the conductor losses maintained a substantial thermal gradient. (For ambient temperatures below some 15 °C, three days loading was not sufficient to even out the pressure difference.)
- Turning off the load caused the pressure in the conductor to drop faster and to a lower level than the pressure under the lead sheath.
- Several days into the no-load part of a cycle, under isothermal conditions and virtually without any pressure gradients in the insulation, the pressure under the lead sheath was steadily declining.

When the temperature of the circulating liquid on day 136 (i.e., four days after the last current turn-off) was reduced from 36 to 8 °C, the pressures recorded under the lead sheath first fell markedly, then increased from around 0.5 bar and up to around 1.0 and 1.4 bar, before they started to slowly decline, see Figure 10 and the expanded view in Figure 12. The observed pressure rise is somewhat unexpected, since lowering the temperature causes the mass to thermally contract, usually leading to a falling pressure. In the conductor in contrast, the temperature reduction caused a distinct pressure drop (from the already low level of 0.3 bar).

4 DISCUSSION

4.1 INTERPRETATION OF PRESSURE PROFILES

The increase in internal pressures observed when heating the cable by passing current is obviously a result of thermal

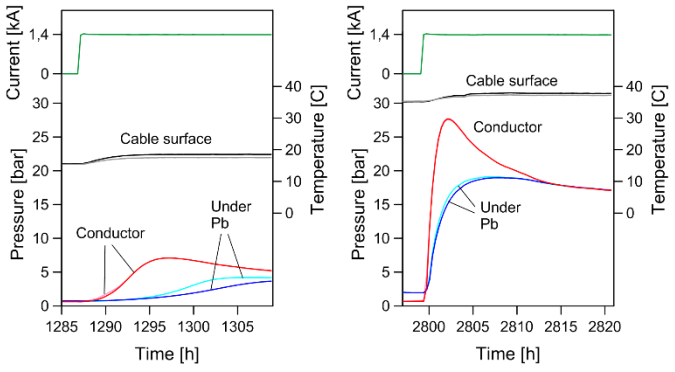

Figure 11. 24–h excerpts from Fig. 10 showing the initial part of the first load cycle with a circulation fluid temperature of 15 °C (left) and 36 °C (right).

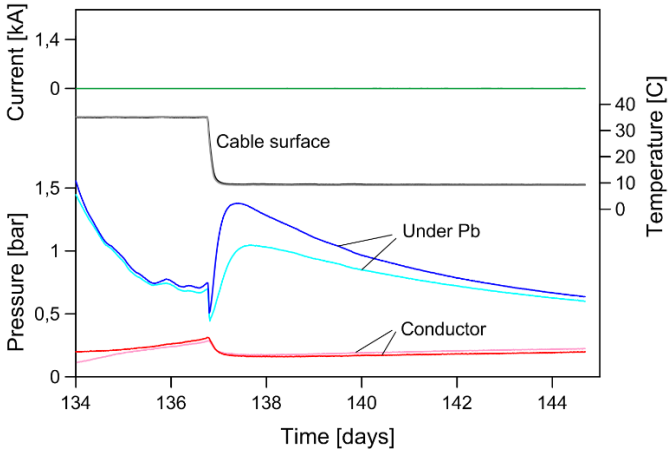

Figure 12. Internal pressure profiles obtained prior to and after reducing the temperature of the circulating liquid from 36 to 8 °C four days after the final load cycle was completed.

This is the accepted version of an article published in IEEE transactions on dielectrics and electrical insulation
http://dx.doi.org/10.1109/TDEI.2019.008522

expansion of the mass. At the lowest temperature levels current loading had little or no effect on the pressure. This is presumably due to the expanding mass filling up any cavities present in the insulation, or that the steel bands not become tensioned at such low temperatures. At higher temperatures the thermal expansion is counteracted by compressive forces generated by the steel bands and to some extent also by the lead sheath, and this causes the internal pressure to increase.

The pressure difference between the conductor and under the lead sheath seen in the first hours of a load cycle is partly due to thermal expansion of the mass and partly caused by the considerably flow resistance through the paper.

Since the temperature in the conductor is around 12 °C higher than at the lead sheath, the thermal expansion and pressure rise in the inner parts of the cable become considerably larger. Hence, the temperature gradient is accompanied by a pressure gradient.

The pressure gradient reached considerable values; in the first test up to more than 30 bar over the 20-mm thick insulation layer. It is reasonable to assume that this generated an outwardly directed radial flow of mass through the paper and the butt gap channels. This gradually altered the mass distribution such that mass probably accumulated under the lead sheath. The flow ceased when the driving force (i. e., the pressure gradient) no longer existed, leaving the cable insulation with a thermal gradient but no pressure gradient for the rest of the three-day loading period.

After the current was switched off, the inner parts of the cable cooled down, and the pressure dropped rapidly as the mass contracted thermally. The resulting pressure had its lowest values at the conductor, as the mass "deficit" here was larger than in the outer insulation layers. The viscosity of the mass was now higher than during current loading because the temperature was lower. (At these temperatures a 10 °C drop roughly triples the viscosity [10].) Moreover, the pressure difference across the insulation was now only around a few bars or less, so the backflow of mass towards the conductor became slow and not sufficient to cancel out the radial pressure difference during the three or four days off periods in the two tests.

When again turning on the load, pressures again rose, but now the difference between the inner and outer layers of the insulation was smaller because of the mass redistribution created during the previous load cycle.

The observation of negative pressures just after load turn-offs (Figure 9) contradicts the common perception that liquids do not take up tensile stresses. However, negative pressures in liquids do exist as a temporary, metastable state. A liquid can sustain a mechanical tension before it eventually cavitates [16]. Evenset measured tensile stresses in MIND cable mass during thermal contraction in confined volumes imminent to the formation of shrinkage cavities [17].

The temporary pressure rise recorded under the lead sheath after reducing the temperature from 36 to 8 °C on day 136 (Figure 12) is somewhat puzzling. It can, however, be explained as a consequence of the steel bands contracting due the rapid cool-down from the outside, thereby compressing the mass film that had been accumulating between the outermost paper layer and the lead sheath. As this mass then began to migrate through the paper layers and into volumes with lower internal pressure, the pressure recorded under the lead sheath fell. Hence, the shape of this pressure profile is determined by the radial mass flow resistance of the paper insulation.

The internal pressure under isothermal conditions – i.e., during the last couple of days of the no-load part of the cycles – was low and almost equal over the entire temperatures range considered. For example, on day 30 the entire cable cross-section was at 3 °C and the internal pressures recordings were in the range 0.3–0.5 bar. On day 135, now with the cable at 35 °C the internal pressures were 0.3–0.7 bar. This is surprising. Thermal expansion and contraction substantially alter the mass volume, and this is expected to be visible in the pressure recordings, particularly as a pressure rise at high temperatures.

Evidently, the internal pressure under isothermal conditions is determined by more factors than temperature alone. These other mechanisms are not easily identified. A slow plastic deformation of the outer layers of the cable (steel bands, lead sheath, PE) would increase or reduce the volume available for the mass-impregnated paper and thus cause the internal pressure to drop or rise. Gas dissolved and released from the mass may yield a similar result. However, neither of these explanations appear clearly convincing. The steel bands are assumed to provide most of the compressive forces, and they are designed to operate in the elastic and not plastic domain. Moreover, the mass is very carefully degassed before it impregnates the cable, so only minute quantities of dissolved gas is available.

Partial discharge measurements on short lengths of MIND cables have shown that current loading caused lasting changes in the dielectric properties [14]. After passing load current it took weeks before the partial discharge behavior returned to what it was before loading. It was concluded that it is not sufficient to assess the dynamic behavior of the insulation system by only considering temperature and space charge distributions. Other mechanisms with longer time constants are also at work. Internal pressure, cavity formation and dielectric strength of MIND cable insulation are closely related quantities. The internal pressure after a load turn-off was here found to be essentially unchanged over an ambient temperature span from 3 to 35 °C. Obviously, the load cycling has also in the present work introduced certain (semi-)permanent changes to the cable, that greatly affect its properties. Identifying the mechanisms behind is clearly important for understanding the limitations of MIND cables under load changes.

4.2 CORRECTNESS OF PRESSURE RECORDINGS

In any short-sample experimental setup supposed to imitate the behavior of an "infinitively" long cable, the cable end fixtures are potential sources for erroneous results. In the present arrangement, the gap between the brass end cup and the insulation was filled with epoxy glue. Ensuring that this interface remains tight when one side is sticky mass-impregnated paper seems difficult. There is a risk that a pressure difference between the inner and outer parts of the

This is the accepted version of an article published in IEEE transactions on dielectrics and electrical insulation
http://dx.doi.org/10.1109/TDEI.2019.008522

insulation will cause mass to flow radially along the cut end surface of the insulation.

If that happens, the measured pressure profiles may possibly resemble those due to mass flow through the bulk of the cable insulation in the rest of the 5-m sample.

However, careful examinations of the measurements reveal no signs of that such an undesired flow at the ends has occurred. The pressure profiles from both cable samples are credible and mutually consistent and have no abrupt and un-explainable incidents that indicate that the pressure difference across the insulation at some point has created a radial "leak" at the end caps.

In any event, the two most important observations from this study (the >30 bar pressure drop across the insulation, and the internal pressure becoming around 1 bar or less a couple of days after a current loading irrespective of the ambient temperature level) are credible. An undesired mass flow through a "short-circuit channel" at the cable ends would not produce such results.

5 CONCLUSION

Thermal expansion of the mass during current loading can cause rather extreme internal pressures (>30 bar) and radial pressure gradients (>1.5 bar/mm) in the insulation of MIND cables. The pressure gradient leads to an outwardly directed flow of mass during loading. After a load turn-off, the pressure drops rapidly. Values below 100 mbar have been measured in the conductor and inner parts of the insulation. The backflow of mass proceeds much slower because the pressure gradient is smaller and the mass viscosity higher.

This radial redistribution of the mass and the low pressures are assumed to influence the dielectric properties of the mass-impregnated paper. The risk of creating harmful shrinkage cavities is believed to increase.

The internal pressure in the insulation became around 1 bar or less when isothermal conditions were reached after a load turn-off, irrespective of whether the ambient temperature was as low as 3 °C or as high as 35 °C. This demonstrates that thermal expansion of the mass is not the sole mechanism determining the internal pressures of MIND cables. Other, still unidentified phenomena are also contributing.

ACKNOWLEDGMENT

This work was supported in part by the Norwegian Research Council, Statnett, Nexans Norway, Fingrid, and Svenska Kraftnät under contract no. 256505/E20.

REFERENCES

[1] T. Worzyk, *Submarine Power Cables: Design, Installation, Repair, Environmental Aspects*, Berlin, Heidelberg, Germany: Springer, 2009.

[2] M. Runde, R. Hegerberg, N. Magnusson, E. Ildstad, and T. Ytrehus, "Cavity formation in mass-impregnated HVDC subsea cables – Mechanisms and critical parameters," IEEE Electr. Insul. Mag., vol. 30, pp. 22-33, 2014.

[3] CIGRÉ Working Group 21-02, "Recommendations for tests of power transmission DC cables for a rated voltage up to 800 kV," Electra, no. 189, pp. 39-55, 2000.

[4] J. Elovaara, U. Jonsson, G. Henning, and E. Peterson, "PD measurements as a tool in upgrading the transmission capacity of the Fenno-Skan HVDC cable," *Int. Council Large Electric Systems (CIGRÉ),* 2002, Paper no. 21-302.

[5] P. Gazzana Priaroggia, P. Metra, and G. Miramonti, "Dielectric phenomena in the breakdown of non pressure assisted, impregnated paper insulated, HVDC cables," Proc. *4th Int. Conf on Cond. Breakdown in Sol. Diel. (ICCBSD)*, 1992.

[6] P. Gazzana Priaroggia, P. Metra, and G. Miramonti, "Research on the breakdown under type test of non-pressurized paper-insulated HVDC cables," European Trans. Electric Power, vol. 3, no. 5, pp. 321-330, 1993.

[7] A. Eriksson, G. Henning, B. Ekenstierna, U. Axelsson, and M. Akke, "Development work concerning testing procedures of mass-impregnated HVDC cables," *Int. Council Large Electric Systems (CIGRÉ),* 1994, Paper no. 21-206.

[8] G. Evenset and G. Balog, "The breakdown mechanism of HVDC mass-impregnated cables," *Int. Council Large Electric Systems (CIGRÉ),* 2000, Paper no. 21-303.

[9] G. Evenset, J. Sletbak, and O. Lillevik, "Cavity formation in mass-impregnated high voltage direct current cable insulation," *Conf. Electr. Insul. Dielectr. Phenom. (CEIDP),* 1998, pp. 554-559.

[10] P. Szabo, O. Hassager, and E. Strøbech, "Modeling of pressure effects in HVDC cables," IEEE Trans. Dielectr. Electr. Insul., vol. 6. pp. 845-851, 1999.

[11] S. Alapati and C. Sonehag, "Electric field behavior in mass impregnated HVDC cable insulation: Effect of cavity formation", *Conf. Electr. Insul. Dielectr. Phenom. (CEIDP),* 2016, pp. 445-448.

[12] I.-S. Kwon, S.-J. Kim, J.-H. Koo, B.-W. Lee, "Time-dependent electric field distribution during load cycle test for HVDC MI cable", *Conf. Electr. Insul. Dielectr. Phenom. (CEIDP),* 2018, pp. 82-85.

[13] Z. Y. Huang, J. A. Pilgrim, P. L. Lewis, S. G. Swingler, and G. Tzemis, "Dielectric thermal-mechanical analysis and constrained high voltage DC cable rating," IEEE Trans. Dielectr. Electr. Insul., vol. 22. pp. 2826-2832, 2015.

[14] M. Runde, O. Kvien, H. Förster, and N. Magnusson "Cavities in mass-impregnated HVDC subsea cables studied by AC partial discharge measurements," IEEE Trans. Dielectr. Electr. Insul., vol. 26, pp. 913-921, 2019.

[15] D.-H. Oh, H.-Y. Lee, S.-J. Kim, B.-W. Lee, "Correlation between partial discharge inception voltage and breakdown voltage characteristics of butt-gap in HVDC mass impregnated PPLP cable," *Conf. Electr. Insul. Dielectr. Phenom. (CEIDP),* 2018, pp. 518-521.

[16] D. H. Trevena, "Cavitation and the generation of tension in liquids," J. Phys D: Appl. Phys., vol. 17, pp. 2139–2164, 1984.

[17] G. Evenset, "Cavitation as a precursor to breakdown of mass-impregnated HVDC cables," PhD dissertation, Norwegian Univ. Science and Technology, Trondheim, Norway, 1999.

This is the accepted version of an article published in IEEE transactions on dielectrics and electrical insulation
http://dx.doi.org/10.1109/TDEI.2019.008522